Berit Jost*, Daniel Coopmann, Christoph Holst and Heiner Kuhlmann

Real movement or systematic errors? – TLS-based deformation analysis of a concrete wall

https://doi.org/10.1515/jag-2022-0041
Received September 27, 2022; accepted January 28, 2023;
published online February 17, 2023

Abstract: Performing deformation analyses with high accuracy demands using terrestrial laser scanners is very challenging due to insufficient knowledge about the error budget and correlations. Terrestrial laser scans suffer from random and systematic errors that degrade the quality of the point cloud. Even though the vast majority of systematic errors can be calibrated, remaining errors or errors that vary with time or temperature influence spatially neighboring points in the same way. Hence, correlations between the measurements exist. Considering area-based deformation analyses, these correlations have two effects: On the one hand, they reduce the effective number of measurements in the point cloud, which mainly influences the decision of whether the movement is significant or not. On the other hand, correlations caused by systematic errors in the scanner can lead to a misinterpretation as a deformation of the object. Within this study, we analyze the deformation of a concrete wall (9.50 m height, 50 m width), and we develop a workflow that avoids the misinterpretation of correlated measurements as deformations of the object. Therefore, we first calibrate the scanner to reduce the influence of systematic errors. Afterwards, we use the average of two-face measurements from several scanner stations to eliminate remaining systematic errors and correlated measurements. This study demonstrates that systematic effects can lead to errors of a few millimeters that are likely to be interpreted as small deformations, and it provides a strategy to avoid misinterpretation. Hence, it is inevitable either to model or to eliminate systematic errors of the scanner while performing a precise deformation analysis with a magnitude of a few millimeters.

***Corresponding author: Berit Jost**, Institute of Geodesy and Geoinformation, University of Bonn, Institute of Geodesy and Geoinformation, Nussallee 17, 53115 Bonn, Germany, E-mail: b.jost@igg.uni-bonn.de
Daniel Coopmann and Heiner Kuhlmann, Institute of Geodesy and Geoinformation, University of Bonn, Nussallee 17, 53115 Bonn, Germany
Christoph Holst, TUM School of Engineering and Design, Technical University of Munich, Chair of Engineering Geodesy, Arcisstraße 21, 80333 Munich, Germany

Keywords: correlations; deformation monitoring; point cloud comparison; stochastic model; terrestrial laser scanner.

1 Introduction

Terrestrial laser scanners (TLS) become more and more popular in engineering geodesy and the field of deformation monitoring [1]. Considering deformations of several centimeters, TLS can reliably detect geometric changes [2]. However, regarding deformations of a few millimeters, the question arises whether the point cloud difference between two epochs is related to geometric changes or caused by systematic errors in the point cloud.

Systematic errors arise due to atmospheric effects, the scanning configuration, the object surface, and systematic misalignments in the scanner [3]. Further errors are related to the registration of multiple scans [1]. Some of these error groups are well studied and can be reduced from the point cloud. Scanner misalignments, for example, can be reduced by calibrating the scanner and applying the calibration parameters to the point cloud [4]. Even though many studies put a lot of effort into the calibration of TLS, the calibration parameters have limited accuracy, they change with time and temperature, and they potentially do not fully describe all systematic errors [5]. Thus, remaining systematic errors still influence the point cloud, and they can be interpreted mistakenly as deformations. Effects due to the scanning geometry or the interaction of the laser beam with the object are subject of current research, but so far, no general evaluation strategy exists [6]. Thus, they cannot be fully quantified and eliminated from the point cloud. This also leads to the fact that the point cloud comparisons that will be shown in the further scope of this paper cannot be reasoned by specific error sources as their individual influences cannot be reproduced. Generally, the errors that cannot be described deterministically should be incorporated into the stochastic model of the point cloud, but so far, it is not possible to represent all errors in the stochastic model [7].

To get an idea of what is due to systematic errors and what is a deformation, this study suggests building the

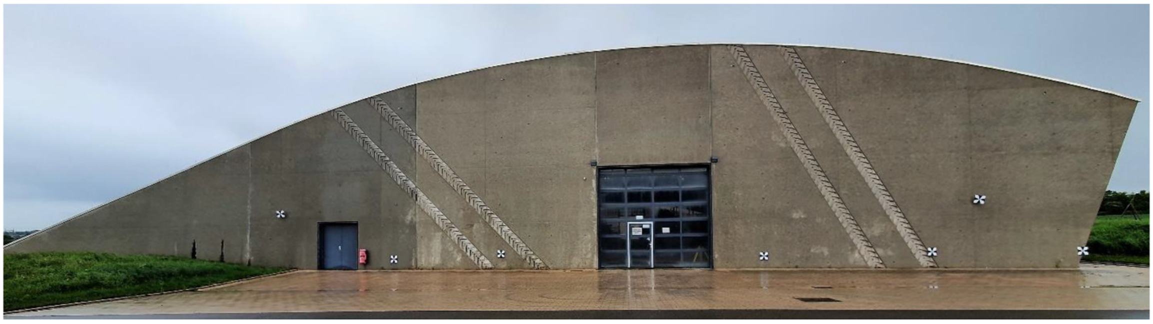

Figure 1: The Bonn Reference Wall.

average of multiple laser scans from different stations and different scanners to reduce the impact of systematic errors as different errors occur due to the scanning geometry and due to different internal misalignments.

Within this study, we scan a concrete wall – the Bonn Reference Wall – with a width of 50 m and a height of 9.50 m (Figure 1) in two epochs to perform an area-based deformation analysis. From Schmitz et al. [8] it is known that the wall moves between 1 and 6 mm over the year.

This study will investigate whether there is a movement between two epochs measured in August and September 2021. Furthermore, it will investigate the possibility of misinterpreting systematic errors as deformations and thus, propose a strategy to reduce this risk. Therefore, the results will be compared to a point-based deformation analysis performed with a total station. Both dates are selected in summer and thus, no high deformation is expected. This choice is used to demonstrate the risk of misinterpreting systematic errors as deformations.

This paper is structured as follows. The theoretical background is given in Section 2. Section 3 presents the data collection and the data processing, while Section 4 presents the results of the deformation analyses and it compares point clouds from different scanners and stations to analyze the relevance of systematic errors. Section 5 discusses the influence of systematic errors within the scanning process and how they can be interpreted as deformations. All findings are summarized in Section 6.

2 Materials and methods

This section recapitulates the theoretical background on which this study is based. It summarizes the error sources in TLS measurements in Section 2.1. Section 2.2 elaborates on the challenges that occur while performing an area-based deformation analysis and Section 2.3 summarizes the methodology to average several point clouds.

2.1 Error sources in TLS measurements

TLSs are polar measuring instruments that acquire the environment with a very high spatial resolution. The scanner measures range, horizontal angle, and vertical angle. From these polar elements, 3D coordinates are derived that represent the point cloud [9]. Panoramic-type scanners, which are used for this study, measure the surrounding with the front and back faces of the scanner. Hence, they only need to rotate 180° around the vertical axis to measure the whole 360° environment. This property can be used to scan in two faces as it is known from total stations [10]. This is done by starting the same scan again with the scanner being rotated by 180°.

Several mechanical requirements are imposed on the instrument, which cannot be completely fulfilled. Hence, systematic errors influence the point cloud, which are, for example, eccentricities and misalignments of the axes, the mirror, or the electro-optical measurement unit [4].

To eliminate the systematic errors from the point cloud, the errors are quantified in a calibration approach and applied to the point cloud. Within this study, we follow the approach of Medić et al. [11]. They determine ten parameters that are relevant for the scanners used in this study. We do not state the single parameters and functional models herein. Therefore, we refer to Medić et al. [11] for more information about the calibration approach. It must be noticed that the calibration parameters may change with time and temperature [5], and that they are only estimated with limited accuracy. Hence, a user calibration can reduce the influence of systematic errors in the point cloud, but it cannot completely eliminate all errors related to internal scanner misalignments.

More systematic errors, which are relevant in this study, are reasoned by the scanning geometry, namely the angle of incidence and the range. Both influence the precision of the rangefinder, which can be described by the backscattered signal strength [12, 13]. However, changing geometries can also lead to systematic effects in the point cloud, for example, due to the surface reflectivity [14] and changing incidence angles [15–17], or the range is measured systematically too short if the incidence angle is high. Atmospheric conditions are often neglected as it does not vary a lot within one scan. However, Friedli [18] demonstrated that refraction errors may occur while measuring long distances.

2.2 Challenges of area-based deformation analysis

Several challenges arise in an area-based deformation analysis that are mainly described in Holst and Kuhlmann [19] and Wunderlich et al.

[20]. One of the main challenges is the establishment of a stochastic model of the point cloud. In general, two epochs are validated for deformations using a global test, which analyses whether points significantly moved or not. This requires the reproduction of measurement points and detailed knowledge of the stochastic model of the measurements [21].

Considering the area-based deformation analysis with TLS, however, it does not fulfil these requirements. On the one hand, single measurement points of the first epoch cannot be reproduced in the second epoch. On the other hand, many studies work on the establishment of an enhanced stochastic model, but the research is not yet completed to use the stochastic model for deformation analyses. Schmitz et al. [7] demonstrated the determination of short-scale correlations in TLS point clouds to build a more comprehensive stochastic model, but long-scale correlations are not considered so far. They are important as they are more likely to be misinterpreted as deformations. For this reason, a classic deformation analysis as proposed for total stations is not yet feasible for area-based deformation analysis.

2.3 Building the average of several point clouds

The general idea of this study is to reduce the amount of systematic errors in TLS point clouds by averaging scans from multiple positions, different scanners, and in two faces. This leads to
- different scan configurations (range, incidence angle, etc.),
- different systematic errors due to different scanner types, and
- a reduction of systematic errors due to two-face measurements as known from total stations.

Generally, building the average of multiple measurements reduces random errors [10]. In our case, we take advantage of the fact that some systematic errors caused by internal misalignments counteract each other using two-face scans, such as the horizontal axis offset (see more in Medić et al. [11]). Furthermore, we assume that although the errors each systematically affect the point cloud, the errors in the point cloud resulting from the superimposition of observations from different scanner locations exhibit behaviour that can be modelled as random. Therefore, the influence of the systematic effects is reduced by averaging.

Before averaging the scans, they are transferred into the same geodetic datum. The averaging is carried out by building a grid of 2 cm over the whole point cloud of the wall and building the median of all points that lie within one grid cell. Hence, there is one representative core point per grid cell, which represents the points of all scans that lie within this grid cell. This is used to average all points of all point clouds that lie within one grid cell with the idea that systematic errors due to different scan configurations and two-face sensitive scanner misalignments are averaged out.

3 Data collection and preparation

To perform the area-based deformation analysis of the Bonn Reference Wall, the wall is scanned in two epochs (August and September 2021). The temperature in August varies between 20 °C and 22 °C, in September it varies between 15 °C and 17 °C. As the impact of systematic errors should

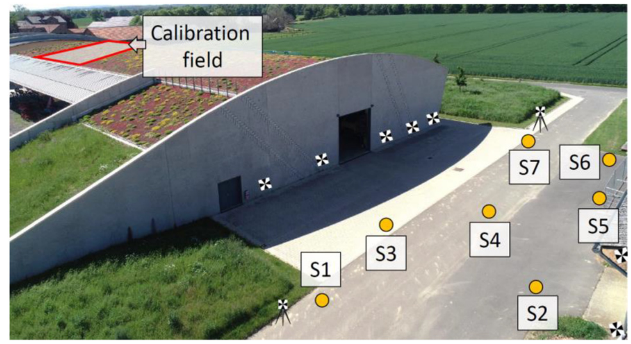

Figure 2: Scanner stations and target distribution in front of the Bonn Reference Wall.

be investigated in this study, the wall is scanned from seven different stations with two different instruments – the Leica ScanStation P50 and the Z + F Imager 5016 (Figure 2). To investigate the impact of systematic errors, and to reduce the impact, two-face measurements are carried out from all stations. This means, 14 scans are acquired per scanner and epoch.

To generate an equal datum for all scans, targets are distributed on the measuring site. Five targets are placed on magnetic nests on the wall, two are fixed on tripods that are centred over ground points, and two targets are affixed to the building opposite the wall (Figure 2). We use BOTA8 (BOnn TArget with 8-fold pattern) as targets that were introduced by Janßen et al. [22].

Inside the machine hall, of which the wall is a part, a calibration field is established. This allows the prompt calibration of the scanners that are used for the monitoring of the wall. Hence, each day of measuring, the scanners are calibrated according to the description given in Medić et al. [11]. Thereby, four scans per scanner are collected within the calibration field. Ten calibration parameters are estimated that are applied to the scans of the wall to reduce systematic errors. After the data acquisition and the calibration, the scans are transformed into one datum using a target-based registration.

To get a reference solution for the deformation analysis, we also monitor the wall with a total station (Leica TS60). Therefore, 17 prisms are mounted to the wall (Figure 3) and measured with a total station from two stations (S2 and S5, Figure 2) to get redundant measurements. The same datum definition as with TLS is used by replacing the targets with prisms.

The object points' coordinates are obtained in a network adjustment with a mean coordinate precision of 0.1 mm in both epochs. Afterwards, the points are tested for deformation using the congruence test. We refrain from

Figure 3: Points for deformation analysis of the wall with the total station Leica TS60.

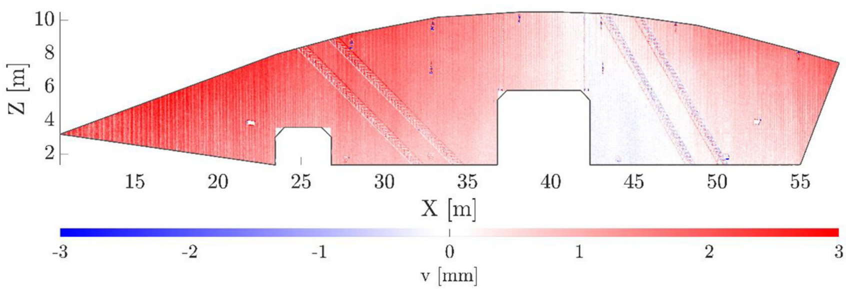

Figure 4: Two-face comparison from S4 for the uncalibrated scans of the Leica ScanStation P50.

giving a detailed description of the data analysis as we strictly follow the point-based deformation analysis [23]. The results are presented in Section 4.6.

4 Results

This section presents the results of this study. It first investigates in how far the calibration can reduce the impact of systematic errors (Section 4.1). Section 4.2 evaluates the systematic errors resulting from the scanning geometry while Section 4.3 investigates the same for different scanners. In Section 4.4 a comparison between the two epochs is carried out for single scans while Section 4.5 compares the averaged point clouds of the two epochs. Section 4.6 presents the results of the total station measurements. All point cloud comparisons are carried out in the software CloudCompare[1] using the multiscale model-to-model cloud comparison (M3C2) [24].

4.1 Impact of the calibration

To reduce the impact of systematic errors, both scanners are calibrated promptly in advance of the measurements in front of the wall. Hence, for each scanner, ten calibration parameters are estimated. The point clouds are corrected according to the description given in Medić et al. [11].

To illustrate the success of the calibration, the two-face measurements are compared to each other. Since most of the calibration parameters are two-face sensitive, they act in opposite directions in the two different faces. For this reason, a two-face comparison can show the improvement of the calibrated point clouds.

Figure 4 presents the two-face comparison of the uncalibrated point clouds acquired from station S4, i.e. in the middle of the wall, with v denoting the M3C2 differences between the point clouds. The scans are carried out with the Leica ScanStation P50. It shows that there is a systematic effect, as there are positive deviations up to 3 mm that increase with a higher vertical angle and higher incidence angle. This is also depicted in Figure 6 (top), which shows the dependency of v on the incidence angle. The red line represents a line approximation through the data. The inclination of the line confirms that v increases with higher incidence angles. In the calibrated case (Figure 5), the deviations are mostly reduced. Moreover, the dependency of v on the incidence angle is reduced (Figure 6, bottom) even though a negative, but absolutely seen lower, inclination (yellow line) is visible, which shows that the dependency is not fully eliminated.

1 https://www.danielgm.net/cc/.

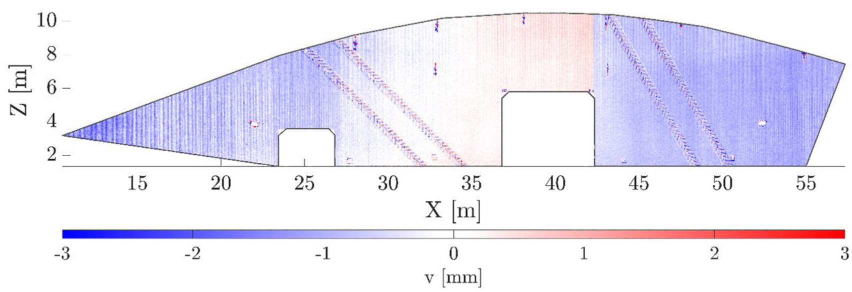

Figure 5: Two-face comparison from S4 for the calibrated scans of the Leica ScanStation P50.

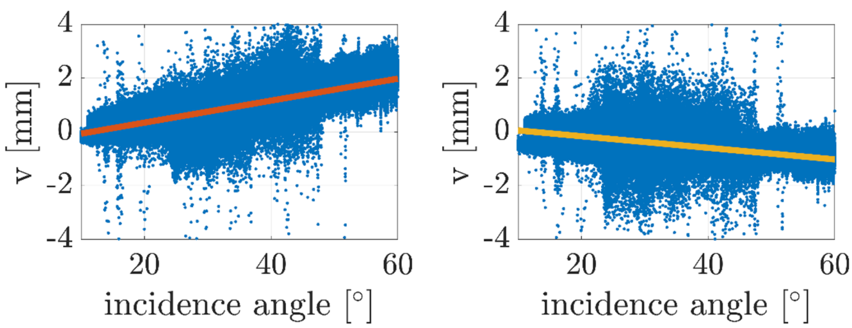

Figure 6: Dependency of the M3C2 differences on the incidence angle. Left: uncalibrated two-face residuals; Right: calibrated two-face residuals. The red and yellow lines represent the corresponding linear trends.

Thus, the calibration reduced the differences between the two faces but it did not succeed to eliminate all systematic errors as there is a strict transition obvious at the right edge of the doorway. This is the transition between the two faces, which visualizes the remaining systematic effects, especially those that affect the point cloud in opposite directions. The limitations of the calibration are described in more detail in Medić [25].

Hence, the calibration already helps to reduce the impact of systematic errors to better interpret the point cloud comparison between two epochs. For this reason, we only use calibrated scans in the further analysis. However, systematic effects remain whose impact will be investigated in the following sections.

4.2 Systematic errors resulting from scan configuration

As mentioned in Section 2.1, the scan configuration plays an important role regarding the errors in TLS point clouds. This means that systematic effects occur due to different ranges and incidence angles. Moreover, as calibration parameters depend on the vertical angle and the range, they impact the point cloud differently using different ranges and vertical angles.

For this reason, comparing two scans of the same object that were collected at almost the same time can have different systematic errors caused by the scanning configuration. It further includes errors resulting from the registration. Figure 7 shows a point cloud comparison between the scans taken from S1 and S7 with the Leica ScanStation P50. Both scans are already calibrated.

Compared to Figure 5, which shows a two-face comparison from the same station, Figure 7 has larger deviations between the two point clouds. This shows that using different scan configurations increases the magnitude of the errors. While the two-face comparison between the calibrated scans has differences in the interval ±1.5 mm, the differences in Figure 7 vary in the range of −3 mm to 1.5 mm.

4.3 Systematic errors resulting from different instruments

In the two latter sections, only scans from the Leica ScanStation P50 have been taken into account. This section evolves the impact of using different laser scanners with different systematic errors due to scanner misalignments. The first comparison also includes the impact of the scan configuration. Therefore, Figure 8 shows the difference between one calibrated scan acquired with the Leica ScanStation P50

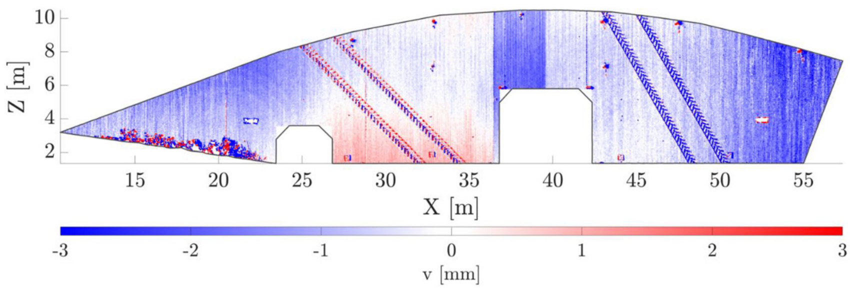

Figure 7: Point cloud comparison between calibrated scans from S1 and S7 collected with the Leica ScanStation P50.

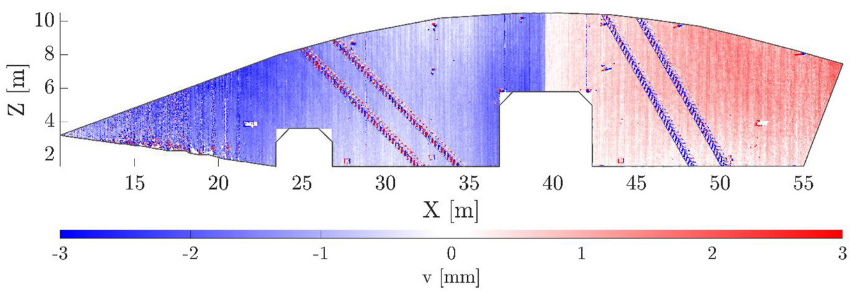

Figure 8: Point cloud comparison between a calibrated scan collected with Leica ScanStation P50 from S1 and a calibrated scan collected with the Z + F Imager 5016 from S7.

from S1 and one calibrated scan acquired with the Z + F Imager 5016 from S7.

Using different scanners increases the magnitude of differences between the compared scans, which vary in the interval of ±3 mm. It is very distinct, that the left part differs negatively and the right part differs positively with a strict border in the middle of the wall. This border indicates the two-face transition of the Imager 5016 at approximately $X = 39$ m. This shows that the calibration could not eliminate all systematic errors for this scanner.

The next comparison disregards the impact of the scanning configuration as both scans are collected from S4 (Figure 9). Again, one scan of the Imager 5016 is compared to one scan of the P50.

This comparison shows that scanning from the same position can significantly reduce the impact of systematic errors as the differences in this comparison vary in the range of −3 mm–1 mm and systematic effects are less distinct compared to Figure 8. The main part of the differences even varies in the interval of ±1 mm, only the left part of the wall, where the incidence angle gets higher for both scans differs more.

Investigating whether different scanners or different scanning configurations cause more systematic errors, we compare Figure 7, which contains the impact of different configurations, to Figure 9, which includes the impact of different scanners. The comparison shows that Figure 9 has slightly smaller deviations and the distribution of the

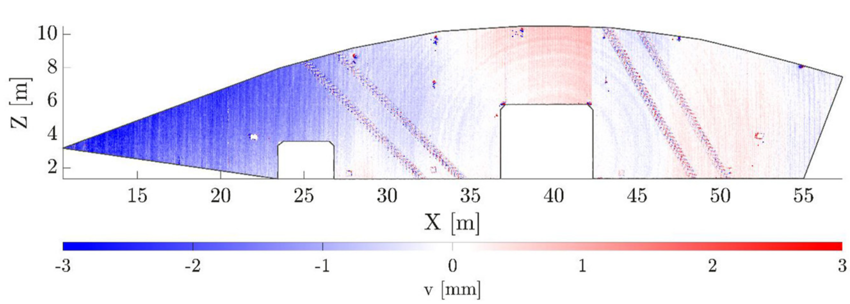

Figure 9: Point cloud comparison between two calibrated scans collected with the Leica ScanStation P50 and the Z + F Imager 5016 from S4.

systematics is less distinct. This shows that scanning with different scanning configurations leads to more systematic errors than scanning with two different instruments from the same station. This conclusion holds for the given scanning geometry and the scanners used in this experiment.

4.4 Point cloud comparison between two epochs

So far, all comparisons have been carried out between scans of one epoch. Now, the different epochs are considered. Therefore, we first compare single scans from two epochs measured from S4. This is done once for the scans of the Leica ScanStation P50 (Figure 10) and once for the calibrated scans of the Z + F Imager 5016 (Figure 11).

Even though both scanners measure in the same epochs, both comparisons are not completely similar. That shows that there are still errors that mitigate the quality of the deformation analysis. Very distinct are the circular deviations, which are most likely cyclic errors [26], which are not calibrated within the calibration approach as their magnitude is very small with up to 0.3 mm. However, both comparisons have differences within a range of 2 mm, which is smaller than in most of the previous comparisons that did not include any deformation.

Thus, all comparisons from Section 4.1 to 4.3 have higher systematic errors than the actual deformation between both epochs. Furthermore, the vast majority of errors can be reduced by calibrating the scanners and scanning from the same position.

However, as both scanners do not provide similar results, these comparisons are not yet satisfying. For this reason, we follow the approach to average multiple point clouds to reduce systematic errors resulting from internal scanner misalignments, the scanning configuration, and the registration.

4.5 Point cloud comparison of the averaged point clouds

This section applies the methodology explained in Section 2.3. In the first step, all 14 scans from the Z + F Imager 5016 are averaged per epoch. This results in two averaged point clouds – one per epoch. Afterwards, the averaged point clouds are compared to each other to perform a deformation analysis. The result is presented in Figure 12.

The same processing is done for the scans of the Leica ScanStation P50 whose results are presented in Figure 13.

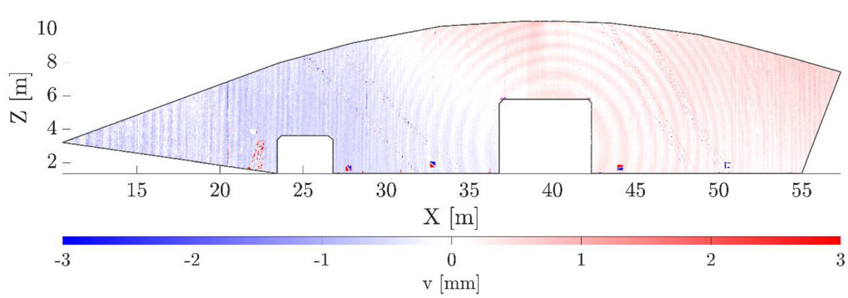

Figure 10: Point cloud comparison between the calibrated scans from the Leica ScanStation P50. One scan is collected in August from S4 and the other one is collected in September from S4.

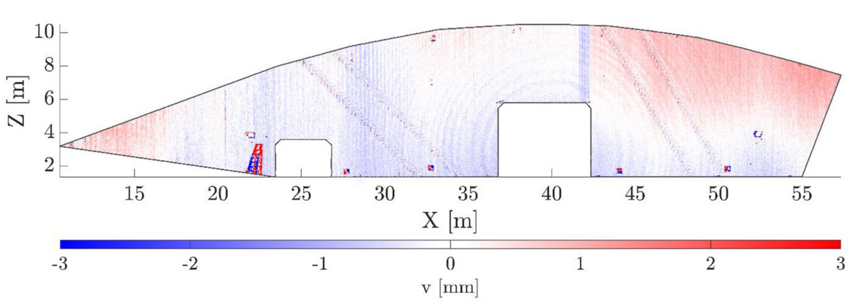

Figure 11: Point cloud comparison between the calibrated scans from the Z + F Imager 5016. One scan is collected in August from S4 and the other one is collected in September from S4.

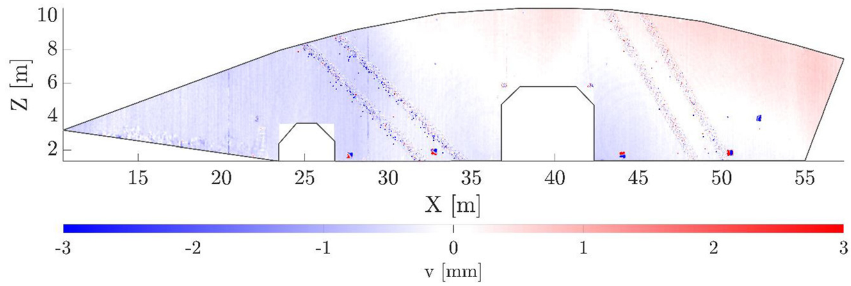

Figure 12: Point cloud comparison between the two averaged point clouds of August and September using all calibrated scans of the Z + F Imager 5016.

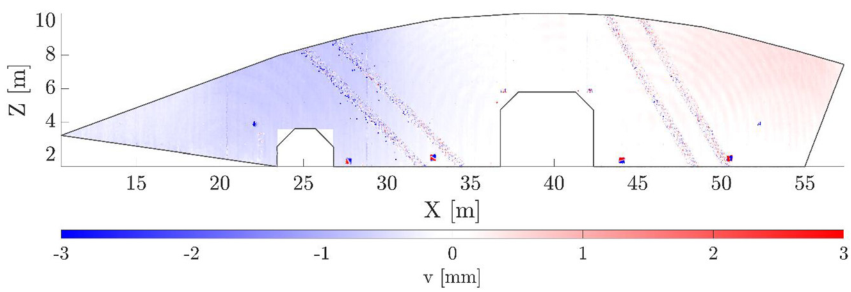

Figure 13: Point cloud comparison between the two averaged point clouds of August and September using all calibrated scans of the Leica ScanStation P50.

The last step is to combine the scans of both scanners and average all 28 scans per epoch. The difference between August and September is presented in Figure 14.

Comparing the three point cloud comparisons in Figures 12–14, we cannot identify big differences between the plots. Figure 12 has slightly more white areas, but all in all the magnitude and distribution of the differences are almost similar. A slight positive tendency is visible in the right part of the wall and the left part slightly differs in the negative direction. The differences in all three comparisons vary within an interval of ±1 mm.

Even though two different scanners are used in Figures 12 and 13, all three figures have the same magnitude and follow the same color pattern. Thus, all the variations that are demonstrated in the previous sections are almost completely averaged out. This indicates that averaging helps to reduce the influence of systematic errors.

Furthermore, the comparison of single scans in Figure 10 also follows the pattern of the three latter shown figures, which indicates that the systematic errors of the Leica ScanStation P50 are already almost reduced using the single scans from S4.

4.6 Results of the point-based deformation analysis

To investigate whether the resulting area-based deformation analysis yields realistic results or not, an point-based deformation has also been performed with a total station. In the deformation analysis, 8 points are indicated that

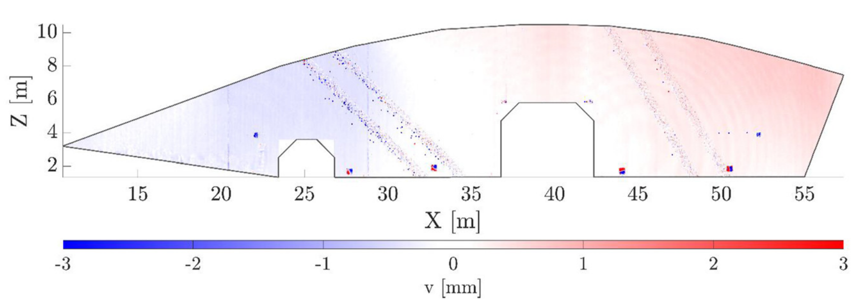

Figure 14: Point cloud comparison between the two averaged point clouds of August and September using all calibrated scans of both scanners.

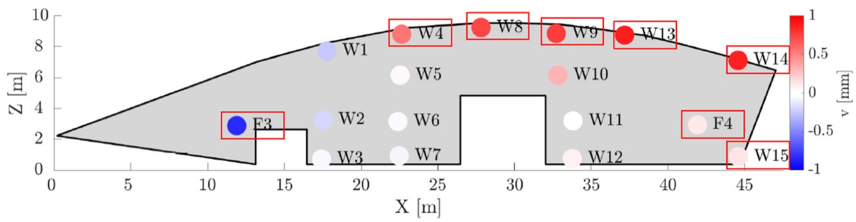

Figure 15: Point-based deformation analysis with significantly deformed points (red squares).

they deformed between the two epochs (red squares in Figure 15). With a magnitude of ±1 mm, the deformation is very small. All points lie at the edge of being significantly deformed or not. Herein, the warmer epoch is subtracted from the cooler epoch. Thus, there is a slight expansion out of the wall with warmer temperatures. The deformation suits the results given in Schmitz et al. [8] who demonstrated that the upper part of the wall moves with varying temperatures.

5 Discussion

This study focuses on the investigation of whether differences in point clouds between two epochs are caused by systematic errors or by a real movement of the object. As, so far, no comprehensive stochastic model for TLS exists, which includes all errors that occur in the measurement, a classic significance analysis cannot be performed. Hence, this study suggests reducing the impact of systematic errors as good as possible to avoid the misinterpretation of those as deformations of the object.

Therefore, laser scans are collected in two epochs. To get a large variety of scans with different scanning configurations, the scanner is placed at seven different stations in front of the object, and all scans are carried out as two-face measurements to also include effects of systematic errors that are two-face sensitive. We further use two different TLS to get individual results that can be compared to each other and on the other hand, both scanners have different systematic errors, i.e. averaging the scans may also reduce more systematic errors. In Section 4, many comparisons have been carried out and the following conclusions can be drawn from the previous analysis:

– Calibration helps to reduce systematic errors, but it cannot eliminate all influences.
– Reproducing the scanning position reduces the impact of systematic errors as the influence due to the scanning configuration is higher than due to different systematic errors resulting from different scanners.
– Building the average of multiple scans further reduces the impact of systematic errors as it reduces the impact of different scan geometries.
– Averaging the scans of two different scanners does not significantly change the result. Hence, it is more worthwhile to scan from more stations than to use different scanners.

Comparing the different scans to each other, it is visible that systematic errors within one epoch can be significantly higher than the error-reduced deformation analysis between both epochs. However, these findings only hold for this object, the chosen scanning configuration, and the scanners that are used.

The question of whether a deformation happened, is not easy to answer. To see the differences between both epochs in more detail, we change the color bar of Figure 14 to ±1 mm in Figure 16.

In this figure, the differences between both epochs are better visible. As the point cloud comparison for the averaged scans of the Z + F Imager 5016 and the Leica ScanStation P50 provide almost the same results, a deformation could have happened within the magnitude of ±1 mm that is indicated in Figure 16. This magnitude is very small for an area-based analysis. A slightly higher deformation would be easier to detect using the presented approach.

To verify the magnitude of deformation, the results of the area-based deformation analysis (Figure 16) are compared to those of the point-based deformation analysis (Figure 15). The magnitude is quite similar between both measurement systems. For a better interpretation, the area between the single points in Figure 15 is interpolated to compare the deformation pattern to the one of the area-based deformation analysis. The result is given in Figure 17.

Comparing Figures 16 and 17, the color pattern looks similar in terms of magnitude and color distribution. This indicates that the deviations in the area-based deformation analysis are not caused by systematic errors coming from the scanning process. However, some systematic effects are still obvious such as the circular rings, which could be

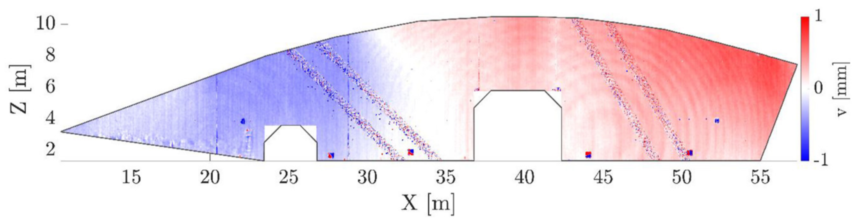

Figure 16: Point cloud comparison between the two averaged point clouds of August and September using all calibrated scans of both scanners (color bar changed to ±1 mm).

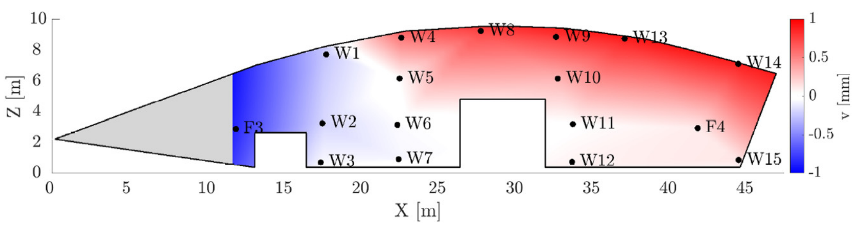

Figure 17: Interpolated results of the point-based deformation analysis.

probably caused by a cyclic error in the instrument. This must be part of future investigations.

6 Conclusions

This study investigates the impact of systematic errors resulting from internal scanner misalignments and the scanning geometry on the point cloud. It further analyzes whether it is possible to reduce the systematic errors in the point cloud to avoid the misinterpretation of those as deformations of the object. This is done by averaging two-face scans from multiple stations and of two different scanners. This study produces the following scientific contributions:

– Systematic errors in TLS point clouds can be reduced by averaging two-face scans from multiple stations and scanners.
– This reduction makes the area-based deformation analysis more sensitive to smaller deformations.

In this study, systematic errors reach up to ±3 mm. Normally, this leads to the assumption that deformations below this magnitude cannot be detected. However, after performing the averaging, the difference between the two epochs only varies between ±1 mm. This magnitude is further confirmed with total station measurements. However, it is still not possible to draw conclusions on the significance of the deviations in the area-based deformation analysis due to an insufficient stochastic model. Nevertheless, the deviations of ±3 mm that are yielded in the beginning, were prevented from being interpreted as deformations by using the averaging method.

Author contribution: All the authors have accepted responsibility for the entire content of this submitted manuscript and approved submission.
Research funding: This work has been partially funded by the Deutsche Forschungsgemeinschaft (DFG, German Research Foundation) under Germany's Excellence Strategy – EXC 2070 – 390732324.
Conflict of interest statement: The authors declare no conflicts of interest regarding this article.

References

1. Lindenbergh R, Pietrzyk P. Change detection and deformation analysis using static and mobile laser scanning. Appl Geomatics 2015;7:65–74.
2. Mukupa W, Roberts GW, Hancock CM, Al-Manasir K. A review of the use of terrestrial laser scanning application for change detection and deformation monitoring of structures. Surv Rev 2017;49:99–116.
3. Soudarissanane S, Lindenbergh R, Menenti M, Teunissen P. Scanning geometry: influencing factor on the quality of terrestrial laser scanning points. ISPRS J Photogrammetry Remote Sens 2011;66:389–99.
4. Lichti DD. Error modelling, calibration and analysis of an AM-CW terrestrial laser scanner system. ISPRS J Photogrammetry Remote Sens 2007;61:307–24.
5. Medić T, Kuhlmann H, Holst C. A priori vs. in-situ terrestrial laser scanner calibration in the context of the instability of calibration parameters. In: Contributions to international conferences on engineering surveying, INGEO & SIG 2020. Dubrovnik, Croatia; 2021.
6. Muralikrishnan B. Performance evaluation of terrestrial laser scanners-a review. Meas Sci Technol 2021;32:072001.

7. Schmitz B, Kuhlmann H, Holst C. Towards the empirical determination of correlations in terrestrial laser scanner range observations and the comparison of the correlation structure of different scanners. ISPRS J Photogrammetry Remote Sens 2021;182:228—41.
8. Schmitz B, Kuhlmann H, Holst C. Deformation analysis of a reference wall towards the uncertainty investigation of terrestrial laser scanners. J Appl Geodes 2021;15:189—206.
9. Vosselman G, Maas HG. Airborne and terrestrial laser scanning. Dunbeath, Scotland, UK: Whittles Publishing; 2010.
10. Schofield W, Breach M. Engineering surveying, 6th ed. Oxford, UK: Elsevier; 2007.
11. Medić T, Kuhlmann H, Holst C. Designing and evaluating a user-oriented calibration field for the target-based self-calibration of panoramic terrestrial laser scanners. Rem Sens 2020;12:15.
12. Wujanz D, Burger M, Mettenleiter M, Neitzel F. An intensity-based stochastic model for terrestrial laser scanners. ISPRS J Photogrammetry Remote Sens 2017;125:146—55.
13. Schmitz B, Holst C, Medic T, Lichti DD, Kuhlmann H. How to efficiently determine the range precision of 3D terrestrial laser scanners. Sensors 2019;19:1466.
14. Zámečníková M, Wieser A, Woschitz H, Ressl C. Influence of surface reflectivity on reflectorless electronic distance measurement and terrestrial laser scanning. J Appl Geodes 2014;8:311—26.
15. Schäfer T. Berührungslose und flächenhafte Deformationsmessungen an Betonoberflächen unter besonderer Berücksichtigung der Interaktion zwischen Laserstrahl und Oberfläche [Ph.D. thesis]. Munich, Germany: Technical University of Munich; 2017.
16. Zámečníková M, Neuner H. Methods for quantification of systematic distance deviations under incidence angle with scanning total stations. ISPRS J Photogrammetry Remote Sens 2018;144:268—84.
17. Linzer F, Papčová M, Neuner H. Quantification of systematic distance deviations for scanning total stations using robotic applications. In: Contributions to international conferences on engineering surveying, INGEO & SIG 2020. Dubrovnik, Croatia; 2021.
18. Friedli E. Point cloud registration and mitigation of refraction effects for geomonitoring using long-range terrestrial laser scanning [Ph.D. thesis]. Zurich, Switzerland: ETH Zurich; 2020.
19. Holst C, Kuhlmann H. Challenges and present fields of action at laser scanner based deformation analyses. J Appl Geodes 2016;10:17—25.
20. Wunderlich T, Niemeier W, Wujanz D, Holst C, Neitzel F, Kuhlmann H. Areal deformation analysis from TLS point cloud — the challenge. Allg Vermess Nachr 2016;123:340—51.
21. Welsch W, Heunecke O. Models and terminology for the analysis of geodetic monitoring observations. In: The 10th FIG international symposium on deformation measurements 2001. Official report of the ad-hoc committee of fig working group 6.1. Orange, California, USA; 2001:390—412 pp.
22. Janßen J, Medic T, Kuhlmann H, Holst C. Decreasing the uncertainty of the target center estimation at terrestrial laser scanning by choosing the best algorithm and by improving the target design. Rem Sens 2019;11:845.
23. Heunecke O, Kuhlmann H, Welsch W, Eichhorn A, Neuner H. Handbuch Ingenieurgeodäsie: Auswertung geodätischer Überwachungsmessungen, 2 Auflage. Heidelberg, Germany: Wichmann; 2013.
24. Lague D, Brodu N, Leroux J. Accurate 3D comparison of complex topography with terrestrial laser scanner: application to the Rangitikei canyon (NZ). ISPRS J Photogrammetry Remote Sens 2013;82:10—26.
25. Medić T. Efficient calibration strategies for panoramic terrestrial laser scanners [Ph.D. thesis]. Bonn, Germany: University of Bonn; 2021.
26. Dorninger P, Nothegger C, Pfeifer N, Molnár G. On-the-job detection and correction of systematic cyclic distance measurement errors of terrestrial laser scanners. J Appl Geodes 2008;2:191—204.